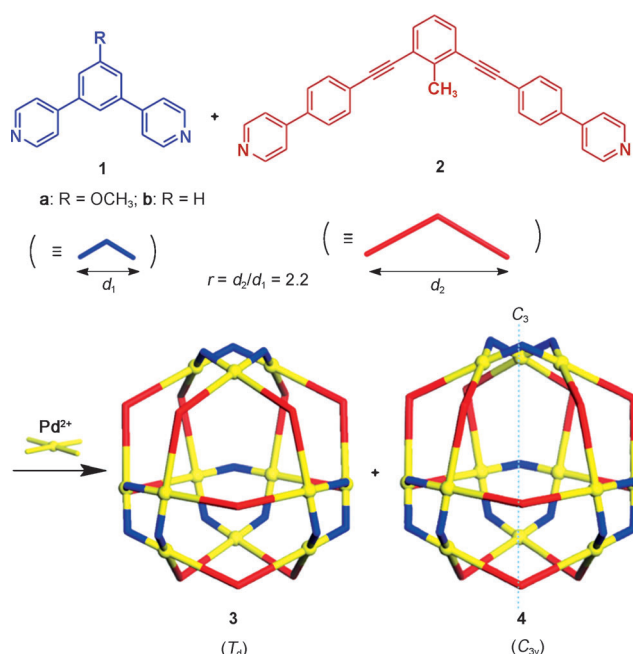


# An $M_{12}(L^1)_{12}(L^2)_{12}$ Cantellated Tetrahedron: A Case Study on Mixed-Ligand Self-Assembly\*\*

Qing-Fu Sun, Sota Sato, and Makoto Fujita\*

**Abstract:** In the self-assembly of  $Pd^{II}$  ions and two different, but similarly shaped, ligands (**1** and **2**), neither random mixing nor self-sorting of the two ligands into two unmixed structures was observed. Instead a mixed, yet sorted,  $Pd_{12}(\mathbf{1})_{12}(\mathbf{2})_{12}$  cantellated tetrahedron (and its pseudoisomer) was selectively formed, thus revealing a fine example of intramolecular self-sorting. A case study showed that a homothetic ratio of  $> 2$  is necessary to observe cantellated tetrahedra.

The self-assembly of giant polyhedral complexes from metal ions and bridging ligands continues to attract considerable interest because it provides an efficient bottom-up approach to afford well-defined nanoscale structures.<sup>[1]</sup> Most polyhedral complexes reported to date contain only one type of ligand, and this results in a simple single product. Self-assembly involving two or more different ligands has often been examined with the aim of generating more elaborate structures and functions, but a clear strategy to predict and account for the structures of mixed-ligand self-assembly does not seem to exist.<sup>[2]</sup> Here we examine the self-assembly of  $Pd^{II}$  ions and two different, but similarly shaped, ligands (**1** and **2**) with a homothetic ratio ( $r$ ) of about 2:1 (Scheme 1). Our previous studies have shown that both ligands give  $M_{12}L_{24}$  cuboctahedral complexes when they are separately complexed with  $Pd^{II}$  ions.<sup>[3]</sup> If the two ligands are randomly mapped onto the edges of a cuboctahedral topology, as many as  $7 \times 10^5$   $Pd_{12}(\mathbf{1})_n(\mathbf{2})_m$  structures (where  $n + m = 24$ ) can in theory be generated (see the Supporting Information for calculations). Despite this large number of possibilities, we observed neither random mixing nor self-sorting into two cuboctahedra, but instead the sole formation of a  $Pd_{12}(\mathbf{1})_{12}(\mathbf{2})_{12}$  cantellated tetrahedron (and its pseudoisomer), in which every  $Pd^{II}$  center coordinates two **1** ligands and two **2** ligands in a *cis* coordination fashion



**Scheme 1.** Self-assembly of regular and pseudocantellated tetrahedra, **3** and **4**, from two similarly shaped ligands **1** and **2**.

(Scheme 1). It is particularly interesting that the selective formation of this mixed, yet sorted, structure provides a fine example of intramolecular self-sorting that differs from the commonly accepted self-sorting, in which two or more ligands assemble orthogonally into their own unmixed structures.<sup>[4]</sup> We also discuss a case study for mixed-ligand self-assembly.

When a 1:1 mixture of **1a** and **2** (4.88  $\mu$ mol each) was added to a solution of  $Pd(BF_4)_2$  (5.66  $\mu$ mol) in  $[D_6]DMSO$  (1.0 mL) and the solution heated at 70 °C for 5 h, reaction mixture showed a relatively simple  $^1H$  NMR spectrum (Figure 1a). Since the spectrum was superimposable on the sum of the spectra of homoleptic  $Pd_{12}(\mathbf{1a})_{24}$  and  $Pd_{12}(\mathbf{2})_{24}$  complexes (**5** and **6**, respectively), our first impression was that the reaction had led to the formation of **5** and **6** through self-sorting. However, ultrahigh-resolution CSI-TOF-MS<sup>[5]</sup> clearly revealed that neither **5** nor **6** was involved in the reaction mixture, but instead a single product with the formula  $Pd_{12}(\mathbf{1a})_{12}(\mathbf{2})_{12}$  was selectively formed. This was indicated by the series of prominent signals for  $[M-(BF_4)_n]^{n+}$ , from which the molecular weight ( $M$ ) was determined to be 11866.70 Da, which is consistent with the  $Pd_{12}(\mathbf{1a})_{12}(\mathbf{2})_{12}$  composition (Figure 1b). DOSY NMR<sup>[6]</sup> spectroscopy also supported the formation of a single product, with a clear single band at  $\log D = -10.43$  ( $D = 3.72 \times 10^{-11} m^2 s^{-1}$ ).

[\*] Dr. Q.-F. Sun, Dr. S. Sato, Prof. Dr. M. Fujita  
Department of Applied Chemistry, School of Engineering  
The University of Tokyo  
Hongo, Bunkyo-ku, Tokyo 113-8656 (Japan)  
E-mail: mfujita@appchem.t.u-tokyo.ac.jp

Dr. Q.-F. Sun  
Present address: State Key Laboratory of Structural Chemistry  
Fujian Institute of Research on the Structure of Matter  
Chinese Academy of Sciences  
155 Yangqiao Road West, Fuzhou, 350002 (P.R. China)

[\*\*] This research was supported by ACCEL, the Japan Science and Technology Agency (JST), and in part by KAKENHI and MEXT (24685010 and 25102007). Synchrotron X-ray diffraction studies were performed at KEK (2009G502 and 2011G522) and SPring-8.

Supporting information for this article is available on the WWW under <http://dx.doi.org/10.1002/anie.201408652>.

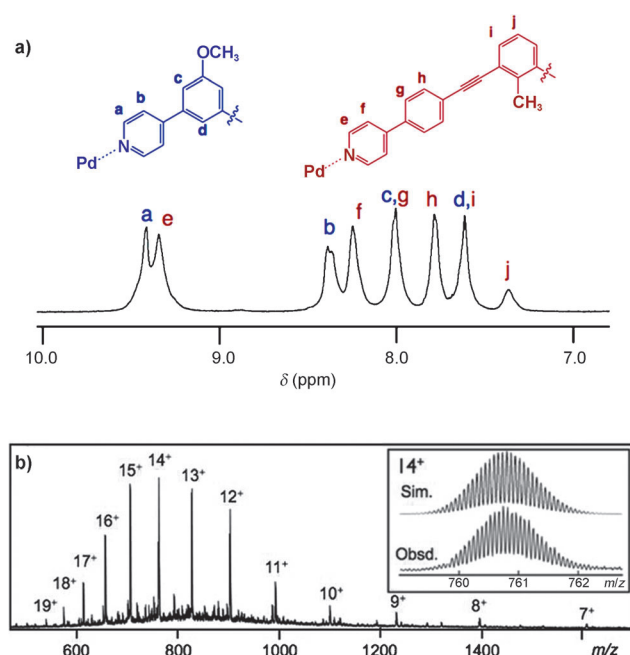


**Figure 1.** a)  $^1\text{H}$  NMR (500 MHz,  $[\text{D}_6]\text{DMSO}$ , 300 K) spectrum of complex **3a/4a** ( $\text{BF}_4^-$  salt). b) CSI-TOF mass spectrum of complex **3a/4a** ( $\text{BF}_4^-$  salt).

As the symmetry of ligands **1a** and **2** are maintained in the  $^1\text{H}$  NMR spectrum, we assumed that the product structure was cantellated tetrahedron **3a** with  $T_d$  symmetry. This structure agrees with the  $\text{Pd}_{12}(\mathbf{1a})_{12}(\mathbf{2})_{12}$  composition and the ligand equivalency in the framework. However, the structure displayed by the crystallographic analysis of its analogue with **1b** instead of **1a** (see Figure 3) was slightly different from our expectation: it was not cantellated tetrahedron **3** but its isomeric structure **4** with the lower  $C_{3v}$  molecular symmetry.<sup>[7]</sup> Structure **4** can be termed a pseudocantellated tetrahedron, and can be generated from cantellated tetrahedron **3** by a  $60^\circ$  rotation of the top small triangular face (Figure 2).

As stated above, the crystallographic analysis was carried out for the product prepared in a similar way from **1b** and **2**. Single crystals of this product (expected to be **3b**) were obtained by slow vapor diffusion of ethyl acetate into a solution of the complex in DMSO. As a consequence of the severe disorder of the anions and solvent molecules, the diffraction power of the crystals remained very low and no decent data could be obtained with the in-house diffractometer. However, satisfactory diffraction data (see the Supporting Information for further details) were collected with synchrotron X-ray sources and the final dataset (to a resolution of  $1.50 \text{ \AA}$ ) was obtained from the NE3Abeamline at KEK Photon Factory. As shown in Figure 3, the structure of the complex displays the  $C_{3v}$  symmetric pseudocantellated tetrahedron framework (**4b**) and contains a huge, solvent-accessible void of  $135582 \text{ \AA}^3$ .<sup>[8]</sup>

Molecular mechanics calculations estimate that **4b** is less stable than **3b** by  $3.0 \text{ kcal mol}^{-1}$ ,<sup>[9]</sup> and thus the hypothetical equilibrium  $\mathbf{3b} \rightleftharpoons \mathbf{4b}$  is in favor of **3b**. Therefore, selective formation of **4b** is unlikely under thermodynamic control.

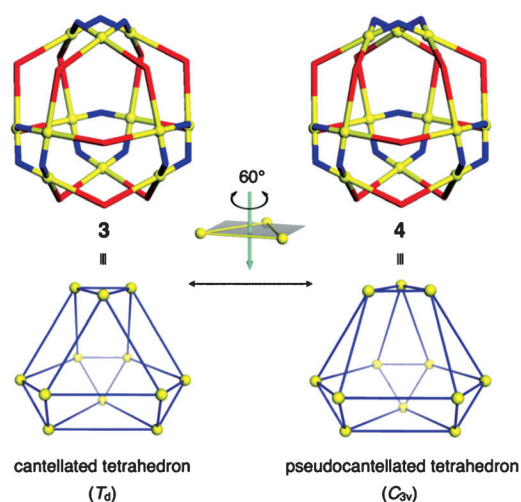


**Figure 2.** Schematic representation of the two isomers of  $\text{Pd}_{12}(\mathbf{1})_{12}(\mathbf{2})_{12}$ : cantellated tetrahedron **3** (left) and pseudocantellated tetrahedron **4** (right). Framework **3** can be converted into **4** by a  $60^\circ$  rotation of one of the small triangular faces. As the substructures of **3** and **4** are different, clearly a conversion from one into another requires a change in the connectivity between the components.

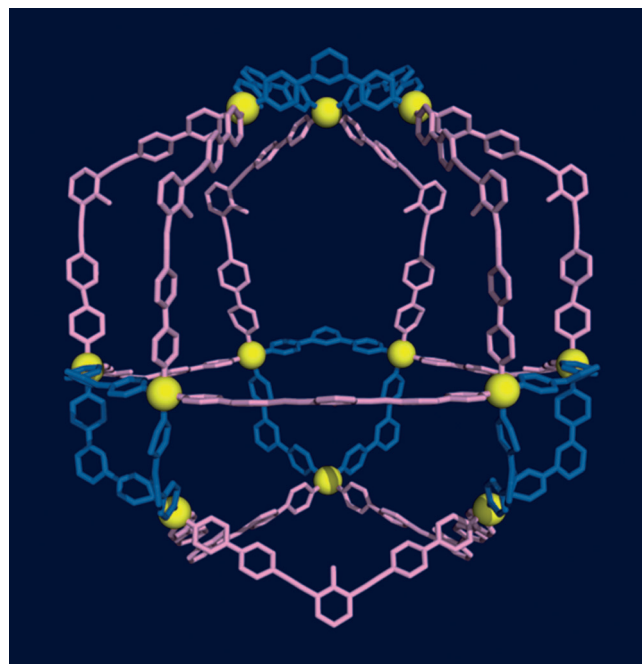


**Figure 3.** Crystal structure of pseudocantellated tetrahedron **4b**. Counterions have been omitted for clarity.

Most probably, a mixture of **3b** and **4b** is formed, but only **4b** crystallizes from the mixed solution. Although ligands **1** and **2** are located in three different positions in **4b**, they are indistinguishable by NMR spectroscopy because of signal broadening and the very similar circumstances of the ligands. Thus, the ratio **3b/4b** cannot be estimated from the NMR spectrum.<sup>[10]</sup>

The heteroleptic self-assembly from similarly shaped ligands is worthy of further discussion. There are three possibilities by which the components are assembled:

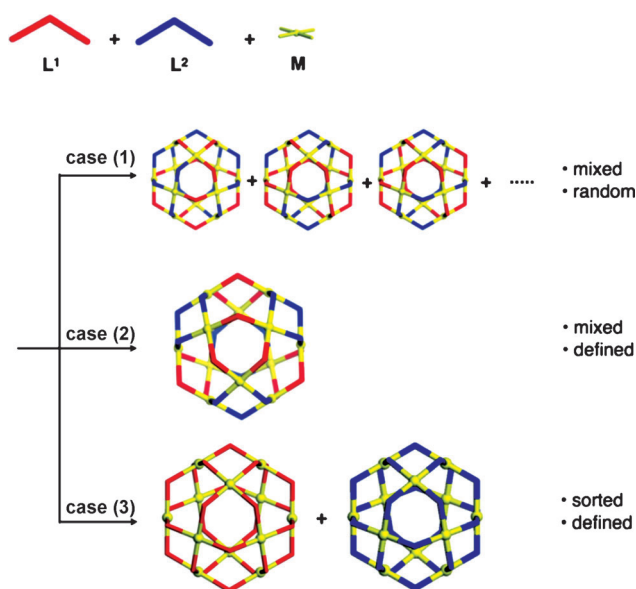


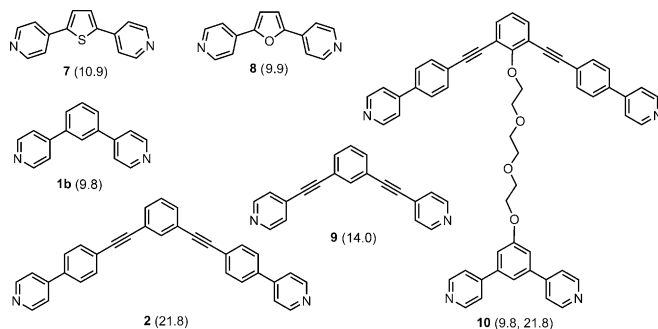
**Figure 4.** Possibilities for heteroleptic self-assembly from two similarly shaped ligands.

1) random mixing, 2) well-defined mixing, and 3) self-sorting (Figure 4). The self-assembly of **3** and **4** from ligands **1** and **2** clearly falls under case (2). We examined several pairs of different ligands to study their manner of self-assembly. Surprisingly, as the ratio of the bridging lengths of the two ligands (defined as  $r$ ) increased, the self-assembly critically switched from case (1) to case (2) (Table 1). We have previously reported that very similar ligands **7** and **8** are statistically incorporated into  $M_{12}L_{24}$  (or  $M_{24}L_{48}$ ) polyhedral frameworks.<sup>[12]</sup> Ligand **9** has a similar shape to **1b**, but its bridging length (14.0 Å) is considerably larger than that of **1b**

**Table 1:** Case study for the heteroleptic self-assembly of two similarly shaped ligands ( $L^1$  and  $L^2$ ).

		$r^{[a]}$	Result
<b>7</b>	<b>8</b>	1.1	case (1) <sup>[b]</sup>
<b>1b</b>	<b>9</b>	1.4	case (1) <sup>[c]</sup>
<b>9</b>	<b>2</b>	1.6	case (1) <sup>[c]</sup>
<b>1b</b>	<b>9</b>	2.2	case (2) <sup>[c]</sup>
<b>10</b>		2.2	case (3) <sup>[d]</sup>

[a]  $r = d_{\text{large}}/d_{\text{small}}$ , where  $d$  defines the N...N distance of the ligands. The  $d$  values, estimated by B3LYP 6-31G(d) or from X-ray data, are given in parentheses below the chemical structures. [b] Ref. [10]. [c] This work. [d] Ref. [3b].



(9.8 Å). When **1b** and **9** were mixed in a 1:1 ratio and treated with  $\text{Pd}(\text{BF}_4)_2$  in  $[\text{D}_6]\text{DMSO}$ , the formation of a statistical mixture was again clearly revealed by CSI-TOF-MS, with prominent signal series corresponding to  $[\text{Pd}_{12}(\text{1b})_m(\text{9})_{24-m}(\text{OTf})_n]^{n+}$  ( $m = 0-12$ ;  $n = 7-13$ ) being observed (see Figure S12 in the Supporting Information). Thus, despite the considerable difference in the lengths ( $r = 1.4$ ), the mixture of **1b** and **9** resulted in statistically distributed mixed-ligand assembly [case (1)], and not well-defined mixed assembly [case (2)]. Similarly, when ligand **2** was complexed with **9** ( $r = 1.6$ ), a statistical mixture was obtained (see Figures S5 and S13 in the Supporting Information). We thus conclude that  $r$  values of 1–1.6 result in self-assembly by case (1), whereas  $r \approx 2.0$  (or larger) leads to self-assembly by case (2). There seems to be a threshold for the switch between cases (1) and (2) at around  $r = 1.6-2.0$ . A sphere-in-sphere structure assembled from covalently linked ligand **10** afforded a fine example of self-sorting [case (3)].

In summary, a mixed-ligand self-assembly process toward regular and pseudocantellated tetrahedra by using a combination of two similarly shaped ligands with distinctly different bridging lengths is provided. It is particularly interesting that, in case (2) self-assembly, two ligands are mixed but are regularly mapped onto the polyhedral framework. This can be described as intramolecular self-sorting, which is different from common self-sorting [case (3)], in that a new well-defined structure arises from the assembly of two different ligands. We expect that intramolecular self-sorting is the first step toward placing multiple functionalities at predetermined positions within giant polyhedral self-assemblies.

## Experimental Section

**Synthesis of 3a/4a ( $\text{BF}_4^-$  salt):** A mixture of ligand **1a** (1.28 mg, 4.88  $\mu\text{mol}$ ) and **2** (2.18 mg, 4.88  $\mu\text{mol}$ ) was treated with  $\text{Pd}(\text{BF}_4)_2$  (1.58 mg, 5.66  $\mu\text{mol}$ ) in  $[\text{D}_6]\text{DMSO}$  (0.991 mL) at 70 °C for 5 h. The complex solution was then directly subjected to NMR spectroscopy and CSI-TOF-MS measurements without any further purification. CSI-TOF-MS revealed that complex **3** was predominantly obtained.  $^1\text{H}$  NMR (500 MHz,  $[\text{D}_6]\text{DMSO}$ , 300 K):  $\delta = 9.38$  (br, 48H), 9.31 (br, 48H), 8.34 (br, 48H), 8.20 (br, 48H), 7.96 (br, 60H), 7.74 (br, 48H), 7.57 (br, 48H), 7.31 (br, 12H), 3.84 (br, 36H), 2.70 ppm (br, 36H). Diffusion coefficient ( $[\text{D}_6]\text{DMSO}$ , 300 K):  $3.72 \times 10^{-11} \text{ m}^2 \text{ s}^{-1}$  ( $\log D = -10.43$ ). CSI-TOF-MS for **3** ( $\text{BF}_4^-$  salt,  $\text{CH}_3\text{CN}$ ): The following signals are those at the highest intensities.  $m/z$  calcd for  $[\text{M}-7(\text{BF}_4^-)]^{7+}$  1608.4853, found 1608.4916; calcd for  $[\text{M}-8(\text{BF}_4^-)]^{8+}$  1396.6741, found 1396.6836; calcd for  $[\text{M}-9(\text{BF}_4^-)]^{9+}$  1231.3764, found 1231.3853; calcd for  $[\text{M}-10(\text{BF}_4^-)]^{10+}$  1099.7384, found 1099.7470; calcd for  $[\text{M}-11(\text{BF}_4^-)]^{11+}$  991.9436, found 991.9484; calcd for  $[\text{M}-12(\text{BF}_4^-)]^{12+}$  901.9480, found 901.9518; calcd for  $[\text{M}-13(\text{BF}_4^-)]^{13+}$  826.0286, found 826.0323; calcd for  $[\text{M}-14(\text{BF}_4^-)]^{14+}$  760.7405, found 760.7448; calcd for  $[\text{M}-15(\text{BF}_4^-)]^{15+}$  704.1575, found 704.1616; calcd for  $[\text{M}-16(\text{BF}_4^-)]^{16+}$  654.7724, found 654.7763; calcd for  $[\text{M}-17(\text{BF}_4^-)]^{17+}$  611.1973, found 611.2012; calcd for  $[\text{M}-18(\text{BF}_4^-)]^{18+}$  572.3528, found 572.3564; calcd for  $[\text{M}-19(\text{BF}_4^-)]^{19+}$  537.7551, found 537.7599.

Single crystal X-ray diffraction data were collected at synchrotron facility (KEK Photon Faculty, beamline NE3A). Despite many attempts to optimize the measurement conditions based on synchrotron radiation, the crystals diffracted very weakly because of the large amount of disordered solvents and anions inside the huge void in the crystal. Finally the crystal was sealed in a glass capillary tube with the

crystallization solvent and measured at ambient temperature to afford the best diffraction data with a resolution of 1.50 Å. Most disordered molecules and residues could not be modeled, and the SQUEEZE<sup>[13]</sup> procedure of PLATON<sup>[8]</sup> was used in the refinement. Crystal data of **4b** (BF<sub>4</sub><sup>−</sup> salt): Space group *Pbcm*, *a* = 55.944(11), *b* = 62.135(12), *c* = 51.308(10) Å, *V* = 178 351(62) Å<sup>3</sup>, *Z* = 4, *T* = 293 K. Anisotropic least-squares refinement for all palladium atoms and isotropic refinement for all the other atoms on 27 878 independent merged reflections (*R*<sub>int</sub> = 0.0766) converged at residual *wR*<sub>2</sub> = 0.3893 for all data; residual *R*<sub>1</sub> = 0.1273 for 27 878 observed data [*I* > 2σ(*I*)], and goodness of fit (GOF) = 1.344. Full experimental details and crystallographic analysis are given in the Supporting Information.

Received: August 28, 2014

Published online: October 7, 2014

**Keywords:** ligand effects · palladium · self-assembly · self-sorting

- [1] a) D. L. Caulder, K. N. Raymond, *Acc. Chem. Res.* **1999**, *32*, 975–982; b) M. Fujita, M. Tominaga, A. Hori, B. Therrien, *Acc. Chem. Res.* **2005**, *38*, 369–378; c) R. Chakrabarty, P. S. Mukherjee, P. J. Stang, *Chem. Rev.* **2011**, *111*, 6810–6918.
- [2] a) S. P. Argent, H. Adams, T. Riis-Johannessen, J. C. Jeffery, L. P. Harding, M. D. Ward, *J. Am. Chem. Soc.* **2006**, *128*, 72–73; b) N. K. Al-Rasbi, I. S. Tidmarsh, S. P. Argent, H. Adams, L. P. Harding, M. D. Ward, *J. Am. Chem. Soc.* **2008**, *130*, 11641–11649; c) J.-R. Li, H.-C. Zhou, *Angew. Chem. Int. Ed.* **2009**, *48*, 8465–8468; *Angew. Chem.* **2009**, *121*, 8617–8620; d) J.-R. Li, H.-C. Zhou, *Nat. Chem.* **2010**, *2*, 893–898.
- [3] a) M. Tominaga, K. Suzuki, M. Kawano, T. Kusakawa, T. Ozeki, S. Sakamoto, K. Yamaguchi, M. Fujita, *Angew. Chem. Int. Ed.* **2004**, *43*, 5621–5625; *Angew. Chem.* **2004**, *116*, 5739–5743; b) Q.-F. Sun, T. Murase, S. Sato, M. Fujita, *Angew. Chem. Int. Ed.* **2011**, *50*, 10318–10321; *Angew. Chem.* **2011**, *123*, 10502–10505; c) D. Fujita, K. Suzuki, S. Sato, M. Yagi-Utsumi, Y. Yamaguchi, N. Mizuno, T. Kumasaka, M. Takata, M. Noda, S. Uchiyama, K. Kato, M. Fujita, *Nat. Commun.* **2012**, *3*, 1093.
- [4] a) A. Wu, L. Isaacs, *J. Am. Chem. Soc.* **2003**, *125*, 4831–4835; b) A. Granzhan, C. Schouwey, T. Riis-Johannessen, R. Scopelliti, K. Severin, *J. Am. Chem. Soc.* **2011**, *133*, 7106–7115; c) J.-F. Ayme, J. E. Beves, C. J. Campbell, D. A. Leigh, *Angew. Chem. Int. Ed.* **2014**, *53*, 7823–7827.
- [5] a) S. Sakamoto, M. Fujita, K. Kim, K. Yamaguchi, *Tetrahedron* **2000**, *56*, 955–964; b) K. Yamaguchi, *J. Mass Spectrom.* **2003**, *38*, 473–490.
- [6] C. S. Johnson, *Prog. Nucl. Magn. Reson. Spectrosc.* **1999**, *34*, 203–256.
- [7] CCDC 1009149 contains the supplementary crystallographic data for this paper. These data can be obtained free of charge from The Cambridge Crystallographic Data Centre via [www.ccdc.cam.ac.uk/data\\_request/cif](http://www.ccdc.cam.ac.uk/data_request/cif).
- [8] A. L. Spek, *Acta Crystallogr. Sect. D* **2009**, *65*, 148–155.
- [9] MM calculations were studied using the module of Forcite on Accelrys Materials Studio software suite with the geometrical optimization on the force field of Universal and the charge calculation of QEq\_charged1.1.
- [10] It is worth pointing out that we cannot fully eliminate the possibility of the selective formation of **4**, which can be reasonably explained by the following hypothesis. Three M<sub>3</sub>L<sub>3</sub> least-numbered cyclic structures are postulated as primary assembly substructures: equilateral triangles, Pd<sub>3</sub>(**1**)<sub>3</sub> and Pd<sub>3</sub>(**2**)<sub>3</sub>, and an isosceles triangle Pd<sub>3</sub>(**1**)(**2**)<sub>2</sub>. The other isosceles triangle Pd<sub>3</sub>(**1**)<sub>2</sub>(**2**) can be ruled out because of its highly distorted structure. The estimated Δ*H* value for the equilibrium between these species (see Scheme S1 in the Supporting Information) is very small (ca. 0.5 kcal mol<sup>−1</sup>). Therefore, the three substructures Pd<sub>3</sub>(**1**)<sub>3</sub>, Pd<sub>3</sub>(**2**)<sub>3</sub>, and Pd<sub>3</sub>(**1**)(**2**)<sub>2</sub> should exist in a roughly 3:2:3 statistical ratio. These initial substructures are connected to form the final structures. Therefore, structure **4**, which includes the three subunit structures in a 4:1:3 ratio, is much more easily formed than **3**, with the three subunits in a 4:4:0 ratio. Once self-assembled, major product **4** is kinetically trapped, because interconversion within its framework is slow.<sup>[11]</sup>
- [11] S. Sato, Y. Ishido, M. Fujita, *J. Am. Chem. Soc.* **2009**, *131*, 6064–6065.
- [12] Q.-F. Sun, J. Iwasa, D. Ogawa, Y. Ishido, S. Sato, T. Ozeki, Y. Sei, K. Yamaguchi, M. Fujita, *Science* **2010**, *328*, 1144–1147.
- [13] A. L. Spek, P. Van Der Sluis, *Acta Crystallogr. Sect. A* **1990**, *46*, 194–201.